Dynamic dislocation modeling by combining Peierls Nabarro and Galerkin methods

Christophe Denoual*
CEA-DAM IdF, Département de physique Théorique et Appliquée, F-91680 Bruyères le Châtel CEDEX, France
(Received 7 October 2003; published 30 July 2004)

A dislocation model combining Peierls Nabarro and Galerkin methods is formulated within the framework of the finite element technique. Complex boundary conditions, dynamic problems, as well as complex dislocation structures can be addressed without any loss in the dislocation core structure description. It is shown that the model reduces to the Peierls Nabarro and phase field techniques under specific limits. An example of a fast moving dislocation dissociated into Shockley partials is given.

DOI: 10.1103/PhysRevB.70.024106 PACS number(s): 61.72.Bb, 61.72.Lk, 61.72.Nn

Dislocation motion and interaction are the main mechanisms that control plasticity of metals. Dislocation core structure is known to strongly influence the applied stress required for dislocation glide[1–3] as well as the mechanism of cross-slip.[4] Though significant results as to crystal stability and dislocation onset[5] were arrived at by other routes, the Peierls-Nabarro model[1–3] (PNM) still remains one privileged tool to calculate core structure, at a remarkably low cost but in a somewhat approximate fashion. Recent use of physical data such as the stacking fault energy[6] as well as the consideration of lattice discreteness[7,8] have, however, strongly improved the predictive capability of PNMs.

In a PNM, core structure emerges from minimizing with respect to the stacking fault vector $\boldsymbol{f}$ the sum of the elastic energy, E^{e}, and the generalized stacking fault energy, $E^{\mathrm{gsf}}(\boldsymbol{f})$ (or γ surface), that represents the displacement jump cost. Input data for E^{gsf} can be obtained from molecular dynamics (MD) calculations (*ab initio*[9] or classical) for a wide range of pressures. Most of the PNM uses one-dimensional (1D) representations of dislocation, even if in some cases 2D dislocation structures can be addressed by a more complex variational formulation (as for screw dislocation cores[10,11] or the onset of a dislocation loop[12,13]). Yet, in spite of its simplicity, the PNM cannot easily handle, e.g., dislocation interaction with a precipitate, Franck–Read sources, junctions, or dynamic loadings. On the contrary, the alternative phase field method (PFM) can deal with the evolution of complex dislocation structures[14–17] as well as with precipitates[18] in anisotropic materials. There, the free energy is minimized with respect to a *phase field* proportional to a displacive *stress free* deformation, leading after minimization to domains of small thickness the border of which are the dislocation lines. So far, however, PFMs can predict the splitting into Shockley partials[17] but are unable to *predict* dislocation core width.

In this paper I introduce a hybrid model combining PNM and a Galerkin Method (GM)[19] that uses E^{gsf} as an input. The model allows for the calculation of core structures *and* dislocation interaction during quasistatic or dynamic (e.g., shock) loadings. It also admits complex boundary conditions and multiple material structures (e.g., dislocation interactions with precipitates). Moreover, for appropriate sets of parameters and for quasistatic loadings, the method is shown to reduce either to a PNM or to a PFM. In the latter case, the use of a modified crystalline energy removes the need for a PFM gradient energy. Contrary to the quasi-continuum method,[20] an exact matching between the Gauss point location and the atomistic structure is not required: the proposed method is mesh-independent.

For clarity, a unique dislocation slip plane S is considered hereafter but the extension to several slip surfaces can be made following Shen and Wang[16] in PFM. Two fields are used in the formulation: a three-dimensional displacement field $\boldsymbol{u}(\boldsymbol{r})$ from which derives the strain, defined in the whole system volume V, and a two-dimensional field $\overline{\boldsymbol{\eta}(\boldsymbol{r})}$ defined on S (upper bars denote 2D vectors expressed in the orthonormal basis $[\boldsymbol{e}^1, \boldsymbol{e}^2]$ which spans S). The field $\boldsymbol{u}(\boldsymbol{r})$ represents a *homogeneous* strain. Displacement discontinuities of PNMs are replaced here by platelet inclusions,[14] and $\overline{\boldsymbol{\eta}(\boldsymbol{r})}$ stands for the *displacement jump* measured when crossing S. The problem consists in minimizing with respect to $\boldsymbol{u}$ and $\overline{\boldsymbol{\eta}}$ the Hamiltonian

$$\mathcal{H} = \int_V \left\{ E^{\mathrm{e}}[\boldsymbol{u}, \overline{\boldsymbol{\eta}}] + \boldsymbol{u} \cdot \boldsymbol{B} + \frac{1}{2}\rho \dot{\boldsymbol{u}}^2 \right\} dV + \int_S E^{\mathrm{isf}}[\overline{\boldsymbol{\eta}}] \mathrm{d}S$$

with $\boldsymbol{B}$ the bulk forces and ρ the material density. E^{e} is the elastic energy density, and E^{isf} is the *inelastic stacking fault energy* (analogous to the so-called "crystalline energy" in PFMs). Thus nonlinearity enters the *constitutive* law through the evolution of the minimizing $\overline{\boldsymbol{\eta}(\boldsymbol{r})}$ as a function of stress. In practice, minimization with respect to the field $\overline{\boldsymbol{\eta}(\boldsymbol{r})}$ is achieved by means of a time dependent Ginzburg Landau equation,[21] whereas the Galerkin method is used to compute the evolution of $\boldsymbol{u}(\boldsymbol{r})$. The energy E^{e} is expressed in terms of the total strain $\varepsilon_{ij} = 1/2(u_{i,j} + u_{j,i})$, the stress-free strain or *inelastic stacking fault strain* $\boldsymbol{\varepsilon}^{\mathrm{isf}}$, and the *local* stiffness tensor $\boldsymbol{K}(\boldsymbol{r})$ as

$$E^{\mathrm{e}}[\boldsymbol{u}, \overline{\boldsymbol{\eta}}] = \frac{1}{2}[\boldsymbol{\varepsilon}(\boldsymbol{r}) - \boldsymbol{\varepsilon}^{\mathrm{isf}}(\boldsymbol{r})] : \boldsymbol{K}(\boldsymbol{r}) : [\boldsymbol{\varepsilon}(\boldsymbol{r}) - \boldsymbol{\varepsilon}^{\mathrm{isf}}(\boldsymbol{r})].$$

The local stiffness $\boldsymbol{K}(\boldsymbol{r})$ will be adjusted within the platelet to a value different from $\boldsymbol{K}^0$, the stiffness in the surrounding bulk homogeneous medium, for reasons to become clear below. For a single slip plane, the stress-free strain $\boldsymbol{\varepsilon}^{\mathrm{isf}}$ reads

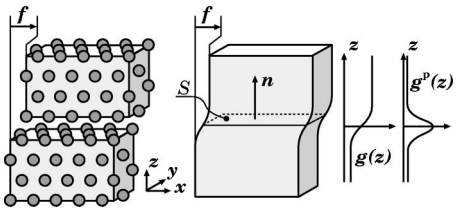

FIG. 1. Continuum (right) or atomistic (left) representation of the Block-Sliding configuration used to calculate E^{gsf}. The slip surface S is the plane $(\boldsymbol{x},\boldsymbol{y})$ and $\boldsymbol{f}$ is a vector of S that stands for the prescribed displacement.

$$\varepsilon_{ij}^{\mathrm{isf}}(\boldsymbol{r}) = \frac{1}{2}[\eta_i(\overline{\boldsymbol{r}})n_j + n_i\eta_j(\overline{\boldsymbol{r}})]\frac{1}{L}g'(\boldsymbol{n}\cdot\boldsymbol{r}/L), \tag{1}$$

where $\boldsymbol{n}$ is the normal to S, $\eta_i(\overline{\boldsymbol{r}}) = \overline{\eta_j}(\overline{\boldsymbol{r}})e_i^j$ and where $\overline{r_i} = e_j^i r_j$ is the projection of $\boldsymbol{r}$ onto S. The function $g(z)$, almost constant everywhere save in the vicinity of $z=0$, defines the spreading of the displacement and is such that $g(+\infty) - g(-\infty) = 1$ and $\int g'^2(z)\mathrm{d}z = 1$. The length scale L is therefore characteristic of displacement field variations. In PFMs, $g'(z)$ is usually taken constant in a platelet of thickness L and equal to zero elsewhere. The specific function used in this work is smoother and determined by the node spacing and the degree of interpolation polynomials. This function $g(z)$ is hard-wired within the Galerkin method but its details are irrelevant here since only the parameter L plays a role in the following.

The crux of the present model is the inelastic stacking fault energy E^{isf} (still undetermined), which depends on material parameters and controls the spreading of dislocation cores. Our only external input is the generalized stacking fault energy, E^{gsf}, assumed to be provided by an independent MD calculation in the nonequilibrium block-sliding BS configuration of Fig. 1, where the strain is localized in the vicinity of the slip surface S. Our concern is to express E^{isf} in terms of L, $\boldsymbol{K}$, and E^{gsf}, and to determine appropriate values for L and $\boldsymbol{K}$. To this aim, the BS configuration, i.e., a nonequilibrium glide of two *rigid* blocks of crystal, is reproduced with the Galerkin method and I require its energy to match E^{gsf} (see Fig. 1). There, the displacement field $\boldsymbol{u}(\boldsymbol{r})$ is *prescribed* in the entire volume and is a function of z only, and the energy in the BS configuration is the sum $E^{\mathrm{e}}+E^{\mathrm{isf}}$ minimized with respect to. $\overline{\boldsymbol{\eta}(\boldsymbol{r})} \equiv \overline{\boldsymbol{\eta}}$, assumed to be constant over the surface S. In the present study, both the total and inelastic stacking fault strain fields derive from the same continuous representation: they are proportional to $g'(\boldsymbol{n}\cdot\boldsymbol{r}/L)$. The elastic strain $\varepsilon - \varepsilon^{\mathrm{isf}}$ then reads

$$\varepsilon_{ij} - \varepsilon_{ij}^{\mathrm{isf}} = \frac{1}{2L}g'\left(\frac{\boldsymbol{n}\cdot\boldsymbol{r}}{L}\right)[(f_i - \eta_i)n_j + n_i(f_j - \eta_j)]. \tag{2}$$

The stiffness tensor is represented as a function of $\boldsymbol{n}\cdot\boldsymbol{r}/L$ only by introducing the tensor $\boldsymbol{K}^{\mathrm{p}}$ of the platelet:

$$\boldsymbol{K}(\boldsymbol{n}\cdot\boldsymbol{r}/L) = \boldsymbol{K}^0 + \boldsymbol{K}^{\mathrm{p}}g^{\mathrm{p}}(\boldsymbol{n}\cdot\boldsymbol{r}/L). \tag{3}$$

Here, $g^{\mathrm{p}}(z)$ is any positive, symmetric function (Fig. 1) with compact support of size w. Since this function is chosen to increase the stiffness *inside* the platelet of width L, I impose $w < L$. The closed-form expression of g^{p}, however, depends on the interpolation technique and is not in the scope of this study. Using Eqs. (2) and (3), the elastic energy by unit surface simplifies into

$$\frac{1}{S}\int_V E^{\mathrm{e}}(\boldsymbol{r})\mathrm{d}V = \frac{1}{2L}(\overline{\boldsymbol{f}} - \overline{\boldsymbol{\eta}})\cdot\boldsymbol{K}^{\mathrm{S}}\cdot(\overline{\boldsymbol{f}} - \overline{\boldsymbol{\eta}}) \tag{4}$$

where $\boldsymbol{K}^{\mathrm{S}} = \boldsymbol{K}^{0\mathrm{S}} + s^{\mathrm{p}}\boldsymbol{K}^{\mathrm{pS}}$, with $K_{ij}^{0\mathrm{S}} = e_m^i n_n e_o^j n_{\mathrm{p}} K_{mnop}^0$, $K_{ij}^{\mathrm{pS}} = e_m^i n_n e_o^j n_p K_{mnop}^p$, and where $s^{\mathrm{p}} = \int g'^2(z)g^p(z)\mathrm{d}z$ is a shape parameter independent of the scale L (a constant for all the simulations). The 2D vector $\overline{\boldsymbol{f}}$ is the restriction to S of the stacking fault vector $\boldsymbol{f}$ ($\overline{f_i} = \boldsymbol{e}^i\cdot\boldsymbol{f}$, $i=1,2$). Imposing the matching requirement between the energies in the BS configuration, namely:

$$E^{\mathrm{gsf}}(\overline{\boldsymbol{f}}) \equiv \min_{\overline{\boldsymbol{\eta}}}\left[\frac{1}{2L}(\overline{\boldsymbol{f}} - \overline{\boldsymbol{\eta}})\cdot\boldsymbol{K}^{\mathrm{S}}\cdot(\overline{\boldsymbol{f}} - \overline{\boldsymbol{\eta}}) + E^{\mathrm{isf}}[\overline{\boldsymbol{\eta}}]\right], \tag{5}$$

and denoting by $\overline{\boldsymbol{\eta}}^*(\overline{\boldsymbol{f}})$ the minimizing value of $\overline{\boldsymbol{\eta}}$, entails the desired relationship:

$$E^{\mathrm{isf}}[\overline{\boldsymbol{\eta}}^*(\overline{\boldsymbol{f}})] = E^{\mathrm{gsf}}(\overline{\boldsymbol{f}}) - \frac{L}{2}\frac{\partial E^{\mathrm{gsf}}}{\partial\overline{\boldsymbol{f}}}\cdot(\boldsymbol{K}^{\mathrm{S}})^{-1}\cdot\frac{\partial E^{\mathrm{gsf}}}{\partial\overline{\boldsymbol{f}}}, \tag{6}$$

with

$$\overline{\boldsymbol{\eta}}^*(\overline{\boldsymbol{f}}) = \overline{\boldsymbol{f}} - L(\boldsymbol{K}^{\mathrm{S}})^{-1}\cdot\frac{\partial E^{\mathrm{gsf}}}{\partial\overline{\boldsymbol{f}}}. \tag{7}$$

Now, a second physical requirement is that for *small strains*, the free energy is given by the linear elasticity law for a volume V surrounding the slip surface:

$$E^{\mathrm{gsf}}(\boldsymbol{f}) = \frac{1}{V}\int_V \varepsilon_{ij}(\boldsymbol{r})K_{ijkl}^0\varepsilon_{kl}(\boldsymbol{r})\mathrm{d}\boldsymbol{r}. \tag{8}$$

Applying it to the BS configuration (which involves a limit $\overline{\boldsymbol{f}}\to 0$) yields the additional condition

$$\frac{\partial^2 E^{\mathrm{gsf}}}{\partial\overline{\boldsymbol{f}}^2}(0) = \frac{1}{L}\boldsymbol{K}^{0\mathrm{S}} \tag{9}$$

from which follows an estimate of L:

$$L = \frac{1}{2}\boldsymbol{K}^{0\mathrm{S}}:\left[\frac{\partial^2 E^{\mathrm{gsf}}}{\partial\overline{\boldsymbol{f}}^2}(0)\right]^{-1}. \tag{10}$$

This derivation shows that L can be seen as a length scale specific to the BS configuration and to the material. It relates E^{gsf} [a configuration- and L-dependent quantity that contains part of an elastic energy, cf. Eq. (5)] to the more intrinsic surface energy E^{isf}.

The inelastic energy defined by Eq. (6) can be considered as a generalized stacking fault energy from which the elastic part has been removed. This splitting is then comparable to the one proposed by Rice[22] with the noticeable difference that the length scale L *naturally emerges* from the minimizing procedure. For aluminum, the characteristic length L de-

duced from (10) is 1.77 Å, 25% less than the separation of the lattice planes (2.34 Å).

For Eq. (6) to define $E^{\mathrm{isf}}(\overline{\boldsymbol{\eta}}^*)$ for all values of $\overline{\boldsymbol{\eta}}^*$, the relationship (7) between $\overline{\boldsymbol{\eta}}^*$ and $\overline{\boldsymbol{f}}$ has to be one-to-one. In other words, whatever $\overline{\boldsymbol{f}}$,

$$\det\left(\frac{\partial \overline{\boldsymbol{\eta}}^*}{\partial \overline{\boldsymbol{f}}}\right) \neq 0. \tag{11}$$

This condition is *a priori* not guaranteed. The only remaining free parameter is the stiffness tensor $\boldsymbol{K}^{\mathrm{p}}$. It should not modify the elastic response excepted for all shear strains in the platelet plane. This can be achieved by taking $\boldsymbol{K}^{\mathrm{p}}$ as a function of the tensor $K^{0\mathrm{S}}$ containing only shear components

$$K^{\mathrm{p}}_{mnop} = \frac{\alpha}{4s_{\mathrm{p}}}(e^i_m n_n + e^i_n n_m)K^{0\mathrm{S}}_{ij}(e^j_o n_p + e^j_p n_o) \tag{12}$$

with $\alpha \geqslant 0$ a scalar proportionality factor. Since $\boldsymbol{e}^i$ and $\boldsymbol{n}$ are unit vectors, $\boldsymbol{K}^{\mathrm{pS}} = (\alpha/s_{\mathrm{p}})\boldsymbol{K}^{0\mathrm{S}}$.

A suitable value of α can in practice always be found to insure condition (11). A choice $\alpha = 0$ [i.e., $\boldsymbol{K}(\boldsymbol{r}) = \boldsymbol{K}^0$] makes the method comparable to the PFM, with three noticeable differences however: (i) the elastic field around the dislocation is obtained by a Galerkin method, thus allowing for computations on any stress field in dynamic loading; (ii) the crystalline energy, here $E^{\mathrm{isf}}(\boldsymbol{\eta})$, is defined as a function of $E^{\mathrm{gsf}}(\boldsymbol{\eta})$ and $\boldsymbol{K}^0$ only; (iii) a gradient energy in the crystalline energy is no longer useful since the dislocation core (and possibly its dissociation into partials) can be resolved. However, the choice $\alpha = 0$ does not allow one to verify Eq. (11) for some materials (e.g., aluminum, see below). If such is the case, the energy E^{isf} is not defined and the method cannot be used. On the other hand, the limit $\alpha \to \infty$ leads to $E^{\mathrm{isf}} = E^{\mathrm{gsf}}$ and $\boldsymbol{\eta} = \boldsymbol{f}$, as stems from Eqs. (7) and (6) with $\boldsymbol{K}^{\mathrm{S}-1} \to \boldsymbol{0}$. The platelet thickness can then be set to 0 (i.e., $L \to 0$), and the method becomes comparable to a PNM, since the elastic and generalized stacking fault energies are minimized with respect to the stacking fault vector $\boldsymbol{f}$.

Since high stiffness slows down the convergence procedure of the TDGL kinetics, the lowest α compatible with Eq. (11) is preferred. Thus the method lies between a PNM and a PFM and the field $\overline{\boldsymbol{\eta}}$ can be attributed no immediate significance. As it is now shown, α does not influence the total energy and therefore does not bias the solution (if considered in terms of the total deformation): it only modifies the partition between elastic and plastic deformations.

For the numerical examples given thereafter, an element free Galerkin (EFG) method[23,24] has been used. One advantage is that the Gauss point locations (from which continuous representation of the fields are derived) can be arbitrary, with no constraint on the node coordination number. Moreover, the interpolation accuracy can be tuned independently by changing the density of nodes or by modifying the polynomial basis degrees. The element free Galerkin method allows for an easy optimization of the mesh density, a feature that is also present in the quasi–continuum method.[20] The computational cost can thus be dramatically reduced compared to a nonoptimized mesh and is not proportional to the simulated volume. Once the mesh is defined, the computational cost does not change and is independent of the dislocation density. In all the following simulations, $s_{\mathrm{p}} = 1/4$.

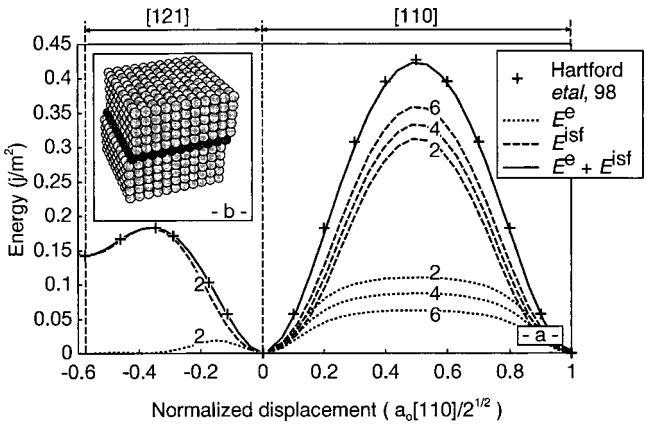

FIG. 2. (a) Energies in the BS configuration (aluminum, with $\boldsymbol{f}$ proportional to [110] right and [121] left). a_0 is the lattice parameter. Different values for α/s_{p} change the partition between elastic and inelastic energies but do not influence the total one. (b) EFG structure to model the BS configuration (nodes are represented by spheres). The darkened spheres are the nodes in the platelet.

The material used is aluminum with the eigenvalues of $\boldsymbol{K}$ (Ref. 25) given by Ref. 26. The energy $E^{\mathrm{gsf}}(\boldsymbol{f})$ has been estimated in the BS configuration by Hartford *et al.*[9] via an *ab initio* calculation, for $\boldsymbol{f}$ proportional to [110] and [121], and with atom relaxation in the $\boldsymbol{z}$ direction (at constant simulation volume). I reconstructed the entire E^{gsf} surface by means of a spline interpolation between these data. The proportionality relationship (9) holds with a maximum relative error of 10% between each component, which insures acceptable compatibility between the *ab initio* (through E^{gsf}) and experimental (through $\boldsymbol{K}^0$) data used. For aluminum, the lowest allowed value of α/s_{p} for the definition of E^{isf} is $\alpha/s_{\mathrm{p}} \approx 2.0$. However, any greater value of α can be used (as demonstrated in Fig. 2) to give the same total energy with, however, different elastic and inelastic energies.

In order to demonstrate that the EFG method can reproduce the generalized stacking fault energy E^{gsf}, the total energy calculated by using the 3D EFG code is plotted in Fig. 2. To reproduce the total energy, the node spacing in the z direction has to be chosen so that the displacement described by the EFG technique is consistent with the definition of the *intrinsic* characteristic scale L. This can be explained by the $1/L$ dependence of the elastic energy in the BS configuration [see Eq. (4)].

There is, however, no such mesh dependence when a dislocation is modeled with the proposed method since the total energy only depends upon *intrinsic* materials properties such as $\boldsymbol{K}^0$, the Burgers vector, and E^{isf}. A comparison between an edge dislocation core structure calculated by the PN model[9] and by the proposed method is presented in Fig 3. This result is quasistatic ($\dot{\boldsymbol{\eta}} = \dot{\boldsymbol{u}} = 0$) and is thus independent of the TDGL kinetics. The splitting into Shockley partials is correctly reproduced and in accordance with other numerical results.[9] Several node spacings have been chosen with no strong influence on the final result except when the mesh becomes too

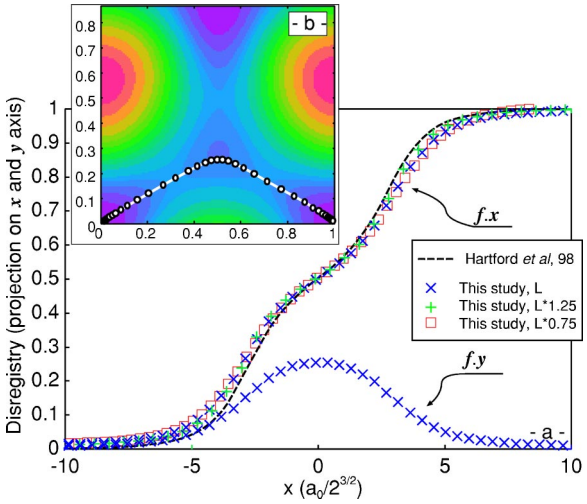

FIG. 3. (Color online) (a) Disregistry components ($\boldsymbol{f}\cdot\boldsymbol{x}$ and $\boldsymbol{f}\cdot\boldsymbol{y}$) for an edge dislocation in aluminum. The modeled structure is a 2D plate of 26.6×26.6 nm^2 with free boundary conditions. The separation into Shockley partials is comparable to the one given by a PNM (Ref. 9). No dependence with respect to the node density (i.e., with the characteristic scale L of the simulation) is found. (b) Disregistry (dots) plotted on the generalized stacking fault energy E^{gsf} in the equilibrium configuration ($x=[\bar{1}10]$, $y=[\bar{1}\bar{1}2]$). The dislocation closely follows the path of minimum energy, except for $\boldsymbol{f}\cdot\boldsymbol{x}\approx0.5$. The white line is a guide for the eye.

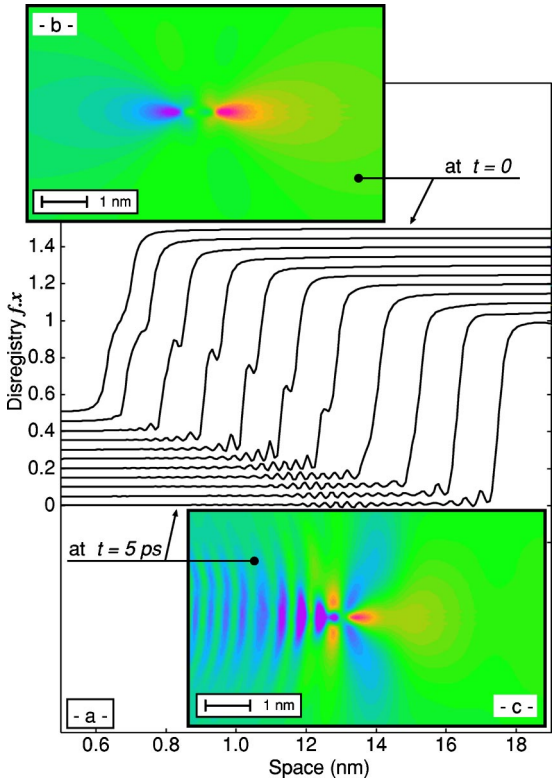

FIG. 4. (Color online) (a) Disregistry component $\boldsymbol{f}\cdot\boldsymbol{x}$ as a function of space plotted each 0.5 ps (curves are shifted vertically to not overlap). The initial dislocation core (splitting into partials) is contracted in less than 5 ps into a narrow one followed by oscillations. (b) and (c) Shear stress (σ_{xz}) of the dislocation (blue$=-2$ Gpa, red$=+4$ Gpa) at $t=0$ (b) and at $t=5$ ps (c). Pictures are cropped and centered on dislocation center.

coarse to correctly represent the dislocation core.

As an illustrative example, the previous dislocation is placed into a rectangular volume in which an initial shear stress of 1 GPa is prescribed. This instantaneous loading makes the dislocation accelerate. The TDGL kinetics is chosen so that minimization with respect to the phase field is achieved at each time step. The initial and final shear stress fields are plotted in Figs. 4(b) and 4(c) as well as the disregistry components $\boldsymbol{f}\cdot\boldsymbol{x}$ [Fig. 4(a)]. The dislocation reaches from the first picosecond a constant velocity of $\approx$2500 m/s, less than 60% of the shear wave celerity for that crystal orientation. The initial splitting into Shockley partials is transformed in less than 2 ps into a complex and asymmetrical core structure in which a strong oscillation takes place [Fig. 4(a)]. The separation into partials eventually vanishes, leading to core contraction as analytical calculations show.[27] The stress field at 5 ps [Fig. 4(c)] shows that the left shear lobe of the "whistling" dislocation is replaced by a zone that gives out in the whole volume a coherent and short wave length signal. However, this first result has to be completed by an analysis of the role of frictional forces (phonon drag) as well as the influence of the discreteness nature of the material at such a length scale (Ref. 28).

This example shows one of the main differences between the proposed method and both PNM/PFM: displacement and disregistry are the minimization result of a functional that contains inertial terms. Unsteady state motion as well as propagating waves are naturally included is this formalism. Another salient difference between the method introduced here and PN methods is that complex microstructures can be considered (precipitate with different stiffness, voids, free boundary conditions…) by only defining the appropriate mesh.

To conclude, the proposed method establishes for the first time a link between Peierls Nabarro and Galerkin methods. This could be achieved only through a careful splitting of the generalized stacking fault energy E^{gsf} (or γ surface) into volume elastic energy and inelastic energy defined on the gliding surface. This allows for an exact reproduction of the γ surface and thus insures a true energetic equivalence with the corresponding *ab initio* calculations. Such a splitting makes the method mesh-independent, provided that the dislocation core can be resolved. This paves the way towards the study of complex dislocation systems within a continuum mechanics framework.

ACKNOWLEDGMENTS

The author thanks Y. P. Pellegrini for valuable discussions and comments on the manuscript. Thanks are also due to S. Christy, F. Pellegrini, O. Coulaud, and J. Roman for having parallelized the code.

*Electronic address: christophe.denoual@cea.fr

[1] R. Peierls, Proc. Phys. Soc. London **52**, 34 (1940).
[2] F. Nabarro, Proc. Phys. Soc. London **59**, 256 (1947).
[3] J. P. Hirth and J. Lothe, *Theory of Crystal Dislocations* (Krieger, New York, 1982).
[4] T. Rasmussen, K. Jacobsen, T. Leffers, O. Pedersen, S. G. Srinivasan, and H. Jónsson, Phys. Rev. Lett. **79**, 3676 (1997).
[5] J. Li, K. J. V. Vliet, T. Zhu, S. Yip, and S. Suresh, Nature (London) **418**, 307 (2002).
[6] V. Vítek, Philos. Mag. **18**, 773 (1968).
[7] B. Joòs and M. S. Duesbery, Phys. Rev. Lett. **78**, 266 (1997).
[8] V. V. Bulatov and E. Kaxiras, Phys. Rev. Lett. **78**, 4221 (1997).
[9] J. Hartford, B. von Sydow, G. Wahnström, and B. I. Lundqvist, Phys. Rev. B **58**, 2487 (1998).
[10] G. Schoeck, Philos. Mag. Lett. **76**, 15 (1997).
[11] A. H. W. Ngan, J. Mech. Phys. Solids **45**, 903 (1997).
[12] G. Xu and A. S. Argon, Mater. Sci. Eng., A **319-321**, 144 (2001).
[13] G. Schoeck, J. Mech. Phys. Solids **44**, 413 (1996).
[14] Y. Wang, Y. Jin, A. Cuitiño, and A. Khachaturyan, Acta Mater. **49**, 1847 (2001).
[15] D. Rodney, Y. L. Bouar, and A. Finel, Acta Mater. **51**, 17 (2003).
[16] C. Shen and Y. Wang, Acta Mater. **51**, 2595 (2003).
[17] C. Shen and Y. Wang, Acta Mater. **52**, 683 (2004).
[18] S. Y. Hu, L. Li, and L. Q. Chen, J. Appl. Phys. **94**, 2543 (2003).
[19] O. C. Zienkiewicz and R. L. Taylor, *The Finite Element Method* (Butterworth-Heinemann, Oxford, 2000).
[20] E. Tadmor, M. Ortiz, and R. Phillips, Philos. Mag. A **73**, 1529 (1996).
[21] P. Hohenberg and B. Halperin, Rev. Mod. Phys. **49**, 435 (1977).
[22] J. R. Rice, J. Mech. Phys. Solids **40**, 239 (1992).
[23] B. Nayrolles, G. Touzot, and P. Villon, Comput. Mech. **10**, 307 (1992).
[24] T. Belytschko, Y. Y. Lu, and L. Gu, Int. J. Numer. Methods Eng. **37**, 229 (1994).
[25] M. M. Mehrabadi and S. C. Cowin, Q. J. Mech. Appl. Math. **43**, 15 (1990).
[26] *American Institute of Physics Handbook*, edited by D. E. Gray (McGraw-Hill, New York, 1963).
[27] J. J. Gilman, Mater. Sci. Eng., A **319-321**, 84 (2001).
[28] C. Denoual, F. Bellencontre, and Y. P. Pellegrini (unpublished).